Dynamic Analysis of Parallel-Link Manipulators Under the Singularity-Consistent Formulation

D.N. Nenchev M. Uchiyama

Department of Aeronautics and Space Engineering
Tohoku University
Aramaki-aza-Aoba, Aoba-ku, Sendai 980-77, JAPAN

Abstract

For a class of parallel-link manipulators we develop a general formulation of the equation of motion, suitable for parallel computations. We analyze the torque requirement when moving through various self-motion type singularities on a path generated under the singularity-consistent framework. The formulation contributes mainly to the analysis of a singularity which is typical for parallel robots only, known from previous studies as "overmobility." We show that if the dynamics of the system is taken under consideration, it is possible to move through such a singularity. This analysis motivates the introduction of the concept of dynamic singularity consistency. As a comprehensive analytical example we use a five bar robotic mechanism.

1. Introduction

A considerable attention in literature has been paid to analyzing singularities of serial-chain robotic mechanisms. In comparison, there is only a limited number of works that analyze singularities of parallel-chain robotic mechanisms [1]–[6]. As far as path planning and control around singularities is concerned, only a few papers are available regarding serial-link manipulators, and there is almost no discussion on this topic for parallel-link devices.

In our previous work [7], [8] we proposed the *singularity-consistent path tracking* approach which guarantees stable motion of a nonredundant robotic mechanism following a pre-specified path that can pass close to, or through, some singularities. In our recent work [9], [10] we applied successfully the above approach to parallel-link manipulators. Especially, we have shown that it is possible to generate feasible paths that would reconfigure the mechanism moving thereby through a so-called instantaneous self-motion singularity. This has been also experimentally verified at our lab with the fast 6 DOF HEXA parallel robot [5], [11]. Other types of singularities, such as dual self-motion and bifurcation, have been also discussed, but the feasibility of motion through them remains to be studied.

The aim of this paper is to introduce a dynamics formulation within the singularity-consistent path tracking framework. This will allow us to accomplish the necessary feasibility study in terms of torque requirements during the motion close to, or through, the singularity. Thereby, we shall focus especially on the dual self-motion singularity.

The paper is organized as follows. In section 2, we present some background on the singularity-consistent formulation for a parallel-link robot. The equation of motion is derived in section 3. Discussion on singularity consistency from dynamical viewpoint can be found in section 4. An analytical example is presented in section 5. Results from a computer simulation are given in section 6. Finally, the conclusion can be found in section 7.

2. Singularity-Consistent Kinematic Formulation for Parallel Robots: Background

It is well known that the kinematic function of a parallel robot is represented as an implicit smooth vector-valued function

$$\boldsymbol{\varphi}(\boldsymbol{p}, \boldsymbol{\theta}_a) = \boldsymbol{0}, \tag{1}$$

reflecting the physical phenomenon of a closed kinematic chain [1], [12]. In the above notation $\boldsymbol{\theta}_a \in \Re^n$ denotes the coordinates of the active joints (the actuated joints), and $\boldsymbol{p} \in \Re^n$ stands for the output-link coordinates[1].

[1] We consider only non-redundant systems.

Proc. IROS 96
0-7803-3213-X/96/ $ 5.00 © 1996 IEEE

Velocity-based control of parallel-link manipulators utilizes the following equation, obtained after differentiation of eq. (1):

$$\mathcal{D}_p\boldsymbol{\varphi}(\boldsymbol{p},\boldsymbol{\theta}_a)\dot{\boldsymbol{p}} + \mathcal{D}_\theta\boldsymbol{\varphi}(\boldsymbol{p},\boldsymbol{\theta}_a)\dot{\boldsymbol{\theta}}_a = \mathbf{0}, \qquad (2)$$

where $\mathcal{D}$ denotes the differential operator. In coordinate form, both differential mappings $\mathcal{D}_p\boldsymbol{\varphi}$ and $\mathcal{D}_\theta\boldsymbol{\varphi}$ are represented by $n \times n$ matrices. Velocity-based control after the above equation degrades severely whenever any of the above mappings, or both, become ill-conditioned.

To avoid the above drawback, we proposed a reformulation of the kinematics under the assumption that the output-link path can be parameterized [9]. Suppose that $\boldsymbol{p} = \boldsymbol{\gamma}(s)$ is the parameterization, where $\boldsymbol{\gamma} : \Re \rightarrow \Re^n$ is a smooth function and the parameter s is not time. Then, the kinematic function is rewritten as:

$$\boldsymbol{\varphi}(\boldsymbol{\gamma}(s),\boldsymbol{\theta}_a) = \mathbf{0}. \qquad (3)$$

After differentiation, we obtain

$$\mathcal{D}_s\boldsymbol{\varphi}(\boldsymbol{\gamma}(s),\boldsymbol{\theta}_a)\dot{s} + \mathcal{D}_\theta\boldsymbol{\varphi}(\boldsymbol{\gamma}(s),\boldsymbol{\theta}_a)\dot{\boldsymbol{\theta}}_a = \mathbf{0}, \qquad (4)$$

where the mapping $\mathcal{D}_s\boldsymbol{\varphi} = \begin{pmatrix} d_1^s & d_2^s & \dots & d_n^s \end{pmatrix}^T$ is an n-dimensional vector-valued function, whereas the mapping $\mathcal{D}_\theta\boldsymbol{\varphi}$ is represented by an $n \times n$ matrix. It is apparent that with this representation, the system's dimension is decreased, as compared to the dimension of the "conventional" equation (2).

For convenience of notation, we augment the active-joint space by the path parameter s:

$$\boldsymbol{q} = \left(s, \boldsymbol{\theta}_a^T\right)^T \qquad (5)$$

and rewrite eq. (3) as

$$\boldsymbol{\eta}(\boldsymbol{q}) = \mathbf{0}, \qquad (6)$$

where $\boldsymbol{\eta} : \Re^{n+1} \rightarrow \Re^n$ is smooth because it is composed of two smooth mappings. Let us introduce a linear local model at $\boldsymbol{q}$:

$$\mathcal{D}_q\boldsymbol{\eta}(\boldsymbol{q})\dot{\boldsymbol{q}} = \mathbf{0}, \qquad (7)$$

where the tangential space mapping $\mathcal{D}_q\boldsymbol{\eta}$ is composed of $\mathcal{D}_s\boldsymbol{\varphi}$ and $\mathcal{D}_\theta\boldsymbol{\varphi}$[2]. In fact, we arrived at a homogeneous $n \times (n+1)$-dimensional system. A set of solutions exists, that can be represented as follows:

$$\dot{\boldsymbol{q}} = b\boldsymbol{\nu}(\boldsymbol{q}), \qquad (8)$$

[2]When not misleading, we shall omit functional dependence.

where b is an arbitrary scalar, and $\boldsymbol{\nu} \in \Re^{n+1}$ is the so-called *null space function.* The system (8) represents an autonomous dynamic system [13]. We point out that the formulation of the type (8) is easily implemented for path planning and control, as shown in our previous work [7], [8]. Since b is arbitrary, it can be determined from the desired motion velocity, as a function of time. The system is decoupled in terms of direction of motion, represented by the null space function $\boldsymbol{\nu}$, and velocity, represented by the scalar variable b.

For a large class of parallel-link manipulators including spatial, such as the HEXA robot, as well as planar ones, such as the five bar mechanism used as the analytical example below[3], we have $\mathcal{D}_\theta\boldsymbol{\varphi}$ =diag$\begin{pmatrix} d_{11}^\theta & d_{22}^\theta & \dots & d_{nn}^\theta \end{pmatrix}$. Then, the *column-augmented system matrix* becomes

$$\mathcal{D}_q\boldsymbol{\eta}(\boldsymbol{q}) = \begin{pmatrix} d_1^s & d_{11}^\theta & & \mathbf{0} \\ d_2^s & & d_{22}^\theta & \\ \dots & & & \ddots \\ d_n^s & \mathbf{0} & & d_{nn}^\theta \end{pmatrix},$$

whereas the null space function is

$$\boldsymbol{\nu}(\boldsymbol{q}) = \begin{pmatrix} v_o & v_1 & \dots & v_n \end{pmatrix}^T, \qquad (9)$$

$$v_0 = \prod_1^n d_{ii}^\theta,\ v_i = -\frac{d_i^s}{d_{ii}^\theta}\prod_1^n d_{ii}^\theta,\ i = 1, ..., n.$$

Note that the division by d_{ii}^θ in the v_i term is used for convenience of notation only.

Based on the above formulation, a comprehensive classification of singularities has been proposed. These include

- instantaneous self-motion singularities;
- dual instantaneous self-motion singularities;
- two types of bifurcation singularities.

Under certain conditions, the instantaneous self-motion may become continuos self-motion. More details can be found in [9], [10].

3. Equation of Motion

Without loss of generality, we shall assume here that the parallel-link manipulator comprises of n serial chains, each of them having one active joint and $n-1$ passive joints, such that the system is statically determined at a non-singular configuration. There are numerous examples that can be described with such a notation including both spatial (e.g. Stewart-platform

[3]See [1] for other examples.

type manipulators and HEXA type ones [5]), as well as a number of planar closed-loop mechanisms.

We denote the joint coordinates of chain i as $\boldsymbol{\phi}_i = \left(\theta_{ai}, \;\; \boldsymbol{\theta}_{pi}^T \right)^T$, where subscripts a and p stand for active and passive, respectively. The serial chain i exerts the wrench $\boldsymbol{w}_i$ on the output link. Thus, the equation of motion can be written as

$$\begin{bmatrix} \tau_{ai} \\ \boldsymbol{0} \end{bmatrix} + \begin{bmatrix} \boldsymbol{J}_{ai}^T(\boldsymbol{\phi}_i) \\ \boldsymbol{J}_{pi}^T(\boldsymbol{\phi}_i) \end{bmatrix} \boldsymbol{w}_i = \tag{10}$$

$$\begin{bmatrix} \boldsymbol{M}_{ai}(\boldsymbol{\phi}_i) \\ \boldsymbol{M}_{pi}(\boldsymbol{\phi}_i) \end{bmatrix} \ddot{\boldsymbol{\phi}}_i + \begin{bmatrix} c_{ai}(\boldsymbol{\phi}_i, \dot{\boldsymbol{\phi}}_i) \\ \boldsymbol{C}_{pi}(\boldsymbol{\phi}_i, \dot{\boldsymbol{\phi}}_i) \end{bmatrix} + \begin{bmatrix} g_{ai}(\boldsymbol{\phi}_i) \\ \boldsymbol{G}_{pi}(\boldsymbol{\phi}_i) \end{bmatrix}$$

$$(i = 1, ..., n),$$

subject to

$$\sum_{i=1}^{n} \boldsymbol{w}_i = \boldsymbol{0}. \tag{11}$$

The notations $\boldsymbol{M}$, $\boldsymbol{C}$, $\boldsymbol{G}$ and $\boldsymbol{J}$ denote parts of the inertia matrix, vector of Coriolis and centrifugal forces, gravity forces, and the Jacobian matrix of the respective serial chain. τ_{ai} is the joint torque which is to be determined. The constraint (11) has been imposed under the assumption that the mass of the output link is distributed and attached to each of the serial chains.

Although the wrenches $\boldsymbol{w}_i, (i = 1, ..., n)$ do not have to be known explicitly, we shall follow here a straightforward procedure that determines them from the lower "p" part of eqs. (10), and using the constraint (11). This yields a system of n^2 equations in n^2 unknowns. The solution of this system (i.e. $\boldsymbol{w}_i$) is then substituted into the upper "a" part of eqs. (10) to finally obtain the torque. The advantage of this approach is twofold: (1) parallel computation is possible, and (2), *dynamic singularities* can be easily identified.

There are several possibilities for solving the above mentioned $n^2 \times n^2$ system. To support computational parallelism, we shall first derive the set of possible wrenches applied through the passive joints of each serial chain. Note that each lower "p" part represents the following underdetermined $(n-1) \times n$ system:

$$\boldsymbol{D}_{pi} = \boldsymbol{J}_{pi}^T(\boldsymbol{\phi}_i)\boldsymbol{w}_i, \tag{12}$$

where

$$\boldsymbol{D}_{pi} = \boldsymbol{M}_{pi}(\boldsymbol{\phi}_i)\ddot{\boldsymbol{\phi}}_i + \boldsymbol{C}_{pi}(\boldsymbol{\phi}_i, \dot{\boldsymbol{\phi}}_i) + \boldsymbol{G}_{pi}(\boldsymbol{\phi}_i) \tag{13}$$

stands for the passive-joint dynamics. The set of possible wrenches for chain i is

$$\boldsymbol{w}_i = \tilde{\boldsymbol{w}}_i + u_i \boldsymbol{n}_i(\boldsymbol{\phi}_i), \tag{14}$$

where $\tilde{\boldsymbol{w}}_i$ denotes a particular solution, u_i is an arbitrary scalar, and $\boldsymbol{n}_i(\boldsymbol{\phi}_i)$ stands for the null space vector of matrix $\boldsymbol{J}_{pi}^T$. Next, we impose the constraint (11):

$$\sum_{i=1}^{n} \tilde{\boldsymbol{w}}_i + \sum_{i=1}^{n} u_i \boldsymbol{n}_i = \boldsymbol{0}, \tag{15}$$

which results in

$$-\tilde{\boldsymbol{w}} = \boldsymbol{N}(\boldsymbol{\phi})\boldsymbol{u}, \tag{16}$$

with $\tilde{\boldsymbol{w}} = \sum_{i=1}^{n} \tilde{\boldsymbol{w}}_i$, $\boldsymbol{w}(\boldsymbol{\phi}) = \left(\boldsymbol{n}_1 \mid \;\; ... \;\; \mid \boldsymbol{n}_n \right)$, and $\boldsymbol{u} = (u_1, ..., u_n)^T$. We shall refer to $\boldsymbol{N}(\boldsymbol{\phi})$ as the null space matrix. The last equation is solved for $\boldsymbol{u}$. Thereafter, each u_i is substituted into eq. (14), and the corresponding wrench $\boldsymbol{w}_i$ is obtained.

The computational advantage of this approach is obvious: instead of solving an $n^2 \times n^2$ system, we solve $n+1$ equations of dimension $n \times n$. n of those equations can be solved in parallel. The determination of the null space vector and the particular solution in eq. (14) requires approximately the same number of operations as needed for the inversion of an $n \times n$ matrix.

The procedure for calculating the torque is summarized as follows. First, we derive the active-joint acceleration $\ddot{\boldsymbol{\theta}}_a$. For this purpose we employ the autonomous equation (8) derived in the previous section under the singularity-consistent framework. As mentioned, b is considered to be a function of the desired velocity on the path, and hence, it is time dependent. Differentiating eq. (8) with respect to time, we obtain

$$\ddot{\boldsymbol{q}} = \dot{b}(t)\boldsymbol{\nu}(\boldsymbol{q}) + b(t)\dot{\boldsymbol{\nu}}(\boldsymbol{q}). \tag{17}$$

$\ddot{\boldsymbol{q}}$ includes the active-joint acceleration. Second, we integrate numerically $\ddot{\boldsymbol{\theta}}_a$ twice to obtain the respective velocity and position. Thereafter, from the kinematic function of the parallel robot, we derive the passive-joint position vector $\boldsymbol{\theta}_p$, which is differentiated twice to obtain the respective velocity and acceleration. Next, the wrenches are obtained as described above. The procedure is completed by substituting the values obtained into the upper "a" part of eqs. (10), and deriving the torques.

4. Singularity-Consistency from the Viewpoint of Dynamics

The procedure outlined in the previous section involves the inversion of matrix $\boldsymbol{N}(\boldsymbol{\phi})$ which is sensitive to singularities. We note, however, that analyzing just the singularities of this matrix is not sufficiently. Obviously, eq. (16) will deliver a feasible solution for vector $\boldsymbol{u}$ and hence for the torque, whenever this equation is *consistent*, and despite the fact that matrix $\boldsymbol{N}(\boldsymbol{\phi})$

is singular. Therefore, one should analyze eq. (16) in terms of consistency. Since vector $\tilde{\boldsymbol{w}}$ which appears on the left side, includes the passive-joint dynamics terms $\boldsymbol{D}_{pi}$, we conclude that the consistency depends upon the dynamics. That is why we speak about a special type of singularity, which can be termed *dynamic singularity of parallel-link manipulators.*

We shall use the dynamic singularity notation to analyze for motion feasibility through the self-motion type singularities (direct task), defined in our previous work [9], [10]. Another potential application would be path planning, in terms of joint positions and their derivatives, to allow for feasible motion through various types of singularities (inverse task). The latter goes beyond the scope of this paper and will be discussed elsewhere.

5. Analytical Example: A Five Bar Robotic Mechanism

Let us consider a five bar mechanism as in Figure 1. Point T is the end-point, a_i, l_i and m_i denote the distance from the origin to the active joint, the arm length, and the rod length, respectively. Further on, we assume that the end-point has to track a straight-line path, parameterized as:

$$\boldsymbol{p} = s\begin{bmatrix}\cos\gamma \\ \sin\gamma\end{bmatrix} + \boldsymbol{p}^{init}, \tag{18}$$

where s is the path parameter, γ denotes the (constant) inclination angle of the path, and $\boldsymbol{p}^{init}$ denotes the end-point coordinates at the initial position. The derivation of the kinematic relations can be found in the appendix.

The null space function of the five bar mechanism is obtained as

$$\boldsymbol{\nu}(\boldsymbol{q}) = \begin{bmatrix} v_0 \\ v_1 \\ v_2 \end{bmatrix} = \begin{bmatrix} d^{\theta}_{11}d^{\theta}_{22} \\ -d^s_1 d^{\theta}_{22} \\ -d^s_2 d^{\theta}_{11}\end{bmatrix}. \tag{19}$$

The singularity analysis of this function revealed the existence of several types of singularities [9], [10]. In this paper, we shall perform the dynamic analysis with regard to only self-motion type singularities. More specifically, it has been shown that whenever:

- either the left or the right kinematic subchain is extended, one of the elements d^{θ}_{ii}, $(i = 1, 2)$ vanishes, yielding the so-called instantaneous self-motion type singularity. The end-point must pause, since the first element of the null space function vanishes ($v_0 = 0$). It is easily seen that with proper path definition, $\exists v_i \neq 0$, $(i = 1, 2)$.
- the two links adjacent to the end-point are aligned, both elements d^s_i, $(i = 1, 2)$ are zero, yielding the so-called dual self-motion type singularity, when the active joints are motionless ($\forall v_i = 0$, $(i = 1, 2)$) but the velocity of the end-point is non-zero ($v_0 \neq 0$), either instantaneously, or continuously.

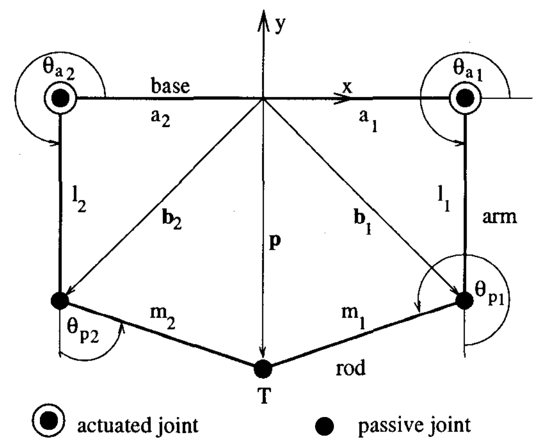

Figure 1. The five bar mechanism.

It is straightforward to derive the time derivative of the null space function, using the following expressions (see the appendix):

$$\dot{d}^s_i(\boldsymbol{q}) = l_i \sin(\gamma - \theta_{ai})\dot{\theta}_{ai} - \dot{s}, \tag{20}$$

and

$$\dot{d}^{\theta}_{ii}(\boldsymbol{q}) = l_i\{\dot{\theta}_{ai}[k_i\cos\theta_{ai} - s\cos(\gamma - \theta_{ai}) - p^{init}_2 \sin\theta_{ai}] + \dot{s}\sin(\gamma - \theta_{ai})\}. \tag{21}$$

This completes the kinematic derivations.

Next, we consider the analysis for dynamic singularities. For each of the two serial chains we have

$$\boldsymbol{J}^T_{pi} = m_i\begin{pmatrix} -\sin\phi_i & \cos\phi_i \end{pmatrix}, \tag{22}$$

where $\phi_i = \theta_{ai} + \theta_{pi}$.

Particular forces acting at the end-point are obtained using the pseudoinverse of the above matrix:

$$\tilde{\boldsymbol{w}}_i = \frac{\boldsymbol{D}_{pi}}{m_i}\begin{pmatrix} -\sin\phi_i & \cos\phi_i \end{pmatrix}^T. \tag{23}$$

The null space is also easily derived as

$$\boldsymbol{n}_i = \begin{pmatrix} \cos\phi_i & \sin\phi_i \end{pmatrix}^T. \tag{24}$$

Dynamic singularities will be analyzed for by looking at the consistency of

$$\begin{bmatrix} \frac{\boldsymbol{D}_{p1}}{m_1}\sin\phi_1 + \frac{\boldsymbol{D}_{p2}}{m_2}\sin\phi_2 \\ -\frac{\boldsymbol{D}_{p1}}{m_1}\cos\phi_1 - \frac{\boldsymbol{D}_{p2}}{m2}\cos\phi_2 \end{bmatrix} =$$

$$\begin{bmatrix} \cos\phi_1 & \cos\phi_2 \\ \sin\phi_1 & \sin\phi_2 \end{bmatrix} \begin{bmatrix} u_1 \\ u_2 \end{bmatrix}. \qquad (25)$$

Whenever the above system is consistent, a proper solution for u_1, u_2 can be obtained, and the actual forces at the end-point will be

$$\boldsymbol{w}_i = (-1)^{i-1}(\tilde{\boldsymbol{w}}_i + u_i \boldsymbol{n}_i). \qquad (26)$$

These forces, substituted into the upper part of the equation of motion, yield directly the joint torque. We point out again that the whole procedure runs in parallel, except when solving the system (25), which is just an 2×2 one.

6. Computer Simulation

The geometry of the mechanism is: $l_i = a_i = 1$ m, $m_i = 1.12$ m. We assume that the links do not have any inertia, and three mass points are assigned to the passive joints as: one at the end-point (1 kg), and two at the passive joints (0.01 kg). We assume also that the linkage is in a horizontal plane, and thus gravity terms are eliminated. The desired path is a straight-line segment with constant slope. The desired path velocity is specified by a constant $b = 1$. In this case, the velocity of the end-point is obtained "naturally", from the curvature of the straight-line-path-induced manifold in augmented joint space.

In the first simulation the initial configuration has been selected as $\theta_{ai}^{init} = -\frac{\pi}{2}$ rad, $p_1^{init} = 0$ m, $p_2^{init} = -1.5$ m. The desired-path slope angle is $\gamma = \frac{3\pi}{4}$ rad. We have studied this sample motion in terms of velocities, in our previous work [9], [10]. Figure 2 shows the result. It is seen that the mechanism moves through several singular configurations. These are self-motion type singularities: (1) denotes the conventional self-motion, while (2) stands for the dual self-motion. First, from the torque graph we see that around the dual self-motion singularity discontinuos torque are generated. These are obviously *not* due to kinematic singularities, since all velocities are very smooth (and also the accelerations, of course). As expected, the reason is the singularity of the null space matrix $\boldsymbol{n}$ *and* the inconsistency of eq. (25). We can conclude that the motion through the dual self-motion singularity on that particular path is not feasible. Second, it is seen that at the conventional self-motion singularities (1) no excessive joint torque are required, and hence, the motion through this type of singularity is feasible. This has been also confirmed from our initial experimental results with the HEXA parallel robot [14].

In the second simulation the desired-path slope angle is modified as $\gamma = \frac{\pi}{2}$ rad. This results in symmetrical motion of both chains, leading to the alignment

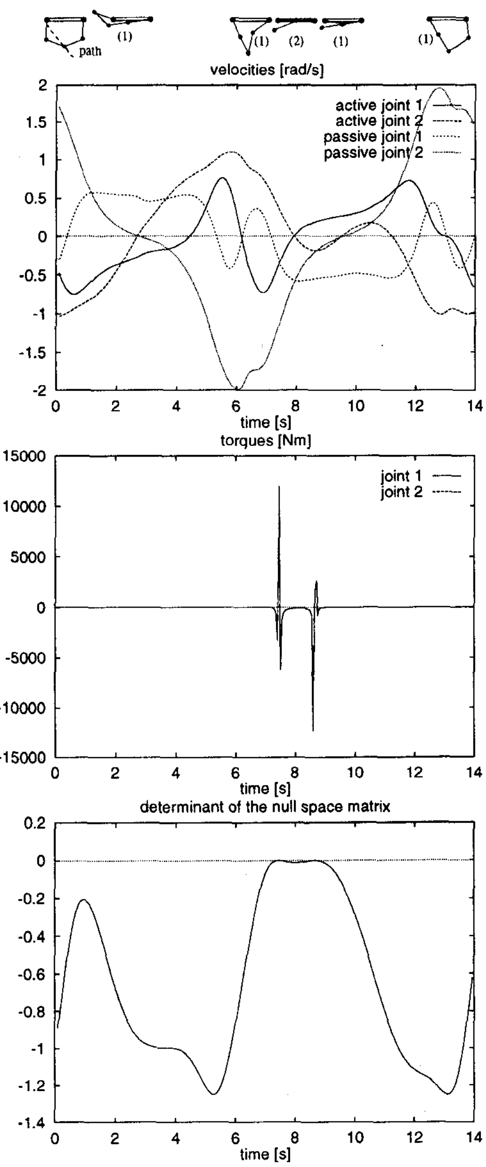

Figure 2. Motion along a straigh-line path with 135 deg inclination.

of the rods (see Figure 3). The configuration represents a dual self-motion singularity in terms of *instantaneous* motion. As seen from Figure 3, the velocities are not excessive, and hence, the discontinuos torque are due to the dynamic singularity. Analyzing this singularity with physical arguments, it is clear that the actuators are not able to generate the necessary end-point forces to support the motion on the desired path. The only thing which can be done at the singularity is just switching the sign of the (maximum) torque. In practice this might be enough to move through the singularity.

In the final simulation the initial configuration is modified with $p_2^{init} = -0.5$ m. Following the same desired-path slope as in the previous case, the linkage encounters another type of singularity, with the two rods overlapping. This is a dual self-motion singularity in terms of continuous motion. The results are shown in Figure 4. It is interesting to note that no excessive torque are required, and the mechanism can move smoothly trough the singularity. This demonstrates the dynamic consistency condition, despite of the singularity of the null space matrix. The joint torque are able to fully support the motion of the end-point on the specified path.

7. Conclusion

We developed a general formulation of the equation of motion of a parallel robot, suitable for parallel computations. Using this formulation, we analyzed the torque requirement when moving through various self-motion type singularities on a path generated under the singularity-consistent framework. The formulation contributes mainly to the analysis of a singularity which is typical for parallel robots only, known from previous studies as "overmobility." We have shown that if the dynamics of the system is taken under consideration, it is possible to move through such a singularity. This analysis motivated the introduction of the concept of dynamic singularity consistency.

Appendix

The i-th element of the kinematic function of the five bar mechanism is derived from the geometrical relation for the i-th kinematic chain:

$$\eta_i(\boldsymbol{q}) \equiv \frac{1}{2}\left(\left\|\overrightarrow{\boldsymbol{b}_i\boldsymbol{p}}\right\|^2 - m_i^2\right) = 0, \qquad (27)$$

where $\boldsymbol{q} = (s,\ \theta_{a1},\ \theta_{a2})^T$ is the augmented joint space vector, $\boldsymbol{b}_i = \begin{bmatrix} (-1)^{i-1}a_i + l_i\cos\theta_{ai} \\ l_i\sin\theta_{ai} \end{bmatrix}$ denotes the vector from the origin to the passive joint connecting the arm and the rod.

Next, we derive the tangential space mappings $\mathcal{D}_s\boldsymbol{\eta}$ and $\mathcal{D}_\theta\boldsymbol{\eta}$:

$$\mathcal{D}_s\boldsymbol{\eta}(\boldsymbol{q}) \equiv \frac{\partial\boldsymbol{\eta}(\boldsymbol{q})}{\partial s} = \begin{bmatrix} (\boldsymbol{p}-\boldsymbol{b}_1)^T \\ (\boldsymbol{p}-\boldsymbol{b}_2)^T \end{bmatrix} \frac{\partial\boldsymbol{p}}{\partial s}, \qquad (28)$$

and each element is

$$d_i^s(\boldsymbol{q}) = k_i\cos\gamma + l_i\cos(\gamma-\theta_{ai}) - s - p_2^{init}\sin\gamma, \quad (29)$$

where $k_i = (-1)^{i-1}a_i - p_1^{init}$. On the other hand, we have

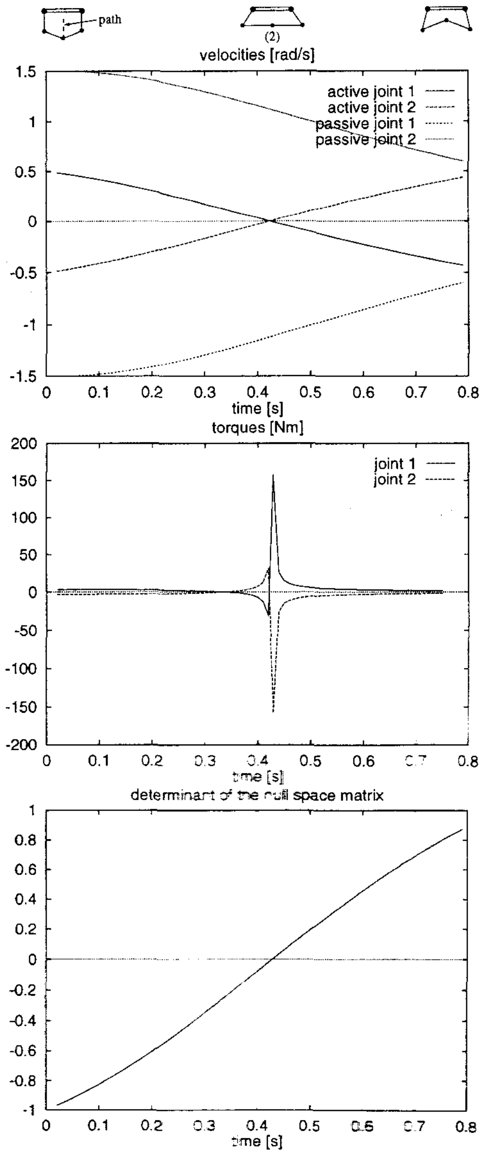

Figure 3. Motion through instantaneous dual self-motion singularity.

$$\mathcal{D}_\theta\boldsymbol{\eta} \equiv \frac{\partial\boldsymbol{\eta}(\boldsymbol{q})}{\partial\boldsymbol{\theta}} = -\begin{bmatrix} (\boldsymbol{p}-\boldsymbol{b}_1)^T\frac{\partial\boldsymbol{b}_1}{\partial\theta_{a1}} & 0 \\ 0 & (\boldsymbol{p}-\boldsymbol{b}_2)^T\frac{\partial\boldsymbol{b}_2}{\partial\theta_{a2}} \end{bmatrix}. \qquad (30)$$

and

$$d_{ii}^\theta(\boldsymbol{q}) = l_i(k_i\sin\theta_{ai} - s\sin(\gamma-\theta_{ai}) + p_2^{init}\cos\theta_{ai}). \qquad (31)$$

References

[1] C. Gosselin and J. Angeles, "Singularity analysis of closed loop kinematic chains," *IEEE Trans. Robotics*

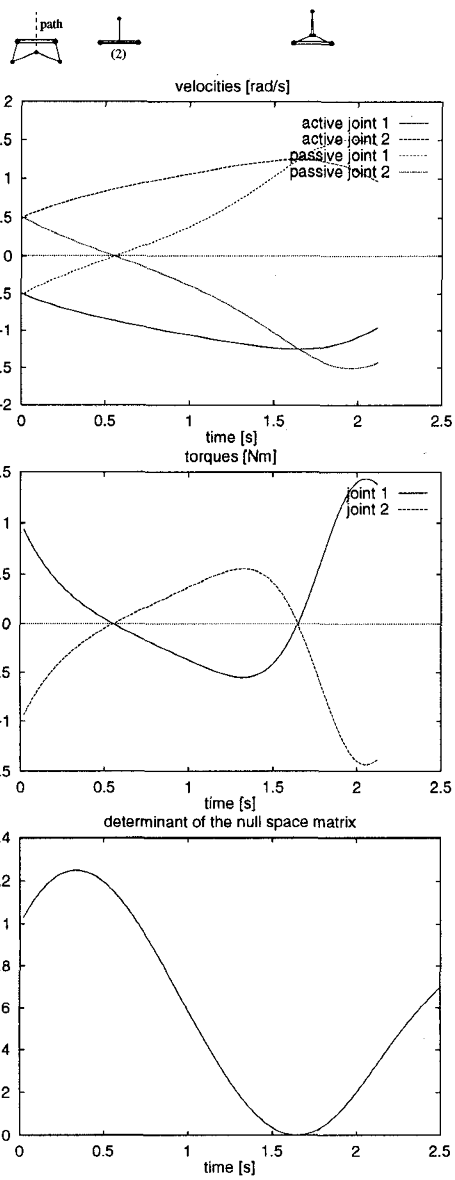

Figure 4. Motion through continuous dual self-motion singularity.

and Automation, Vol. 6, No. 3, pp. 281–290, June 1990.

[2] S. Lee and S. Kim, "Kinematic feature analysis of parallel manipulator systems," in *Proc. 1994 IEEE Int. Conf. Robotics and Automation*, San Diego, California, May 1994, pp. 77–82.

[3] O. Ma and J. Angeles, "Architecture singularities of platform manipulators," in *Proc. 1991 IEEE Int. Conf. Robotics and Automation*, Sacramento, California, April 9–11, 1991, pp. 1542–1547.

[4] J.P. Merlet, "Singular configurations of parallel manipulators and Grassman geometry," *The Int. Journal of Robotics Research*, Vol. 8, No. 5, pp. 45–56, 1989.

[5] F. Pierrot, M. Uchiyama, P. Dauchez and A. Fournier, "A new design of a 6-DOF parallel robot," *Journal of Robotics and Mechatronics*, Vol. 2, No. 4, pp. 92–99, 1989.

[6] D. Zlatanov, R.G. Fenton, and B. Benhabib, "Singularity analysis of mechanisms and robots via a velocity-equation model of the instantaneous kinematics," in *Proc. 1994 IEEE Int. Conf. Robotics and Automation*, San Diego, California, May 1994, pp. 986–991.

[7] D.N. Nenchev and M. Uchiyama, "Singularity consistent path tracking: a null-space based approach," in *Proc. 1995 IEEE Int. Conf. Robotics and Automation*, Nagoya, Japan, May 21–27, 1995, pp. 2482–2489.

[8] D.N. Nenchev, "Tracking manipulator trajectories with ordinary singularities: a null space based approach," *The Int. J. of Robotics Research*, Vol. 14, No. 4, pp. 399–404, 1995.

[9] D.N. Nenchev and M. Uchiyama, "Singularity analysis and singularity-consistent path planning and control of parallel-link manipulators," *Int. Symp. on Microsystems, Intelligent Materials and Robots*, Sendai, Japan, Sept. 27-29, 1995, pp. 576–579.

[10] D.N. Nenchev and M. Uchiyama, "Singularity-consistent path planning and control of parallel robot motion through instantaneous self-motion type singularities," in *Proc. 1996 IEEE Int. Conf. Robotics and Automation*, Minneapolis, Minnessotta.

[11] M. Uchiyama, K. Iimura, F. Pierrot, P. Dauchez, K. Unno and O. Toyama, "A new design of a very fast 6-DOF parallel robot," in *Proc. 23rd Int. Symposium on Industrial Robots (ISIR)*, Barcelona, Spain, Oct. 6–9, 1992, pp. 771–776.

[12] V.B. Zamanov and Z.M. Sotirov, "Duality in mechanical properties of sequential and parallel manipulators," in *Proc. 20th Int. Symposium on Industrial Robots (ISIR)*, Tokyo, Japan, Oct. 4–6, 1989, pp. 1041–1050.

[13] D.N. Nenchev and M. Uchiyama, "Singularity consistent velocity command generation for nonredundant robots," in *Proc. 1995 Int. Conf. on Advanced Robotics (ICAR)*, Sant Feliu de Guixols, Spain, Sept. 20–22, 1995, pp. 71–78.

[14] D. Nenchev et al, "Singularity-consistent control of nonredundant robots," Video Proceedings of the *1996 IEEE Int. Conf. Robotics and Automation*, Minneapolis, Minnesota, April 22–28, 1996.